

**MODELING OF NONLINEAR MATERIAL BEHAVIOR IN MICROSTRUCTURALLY  
ENGINEERED FERROELECTRIC CERAMICS**

**Joshua Robbins**

Multiscale Dynamic Material Modeling  
Sandia National Laboratories  
Albuquerque, New Mexico, 87123  
Email: [jrobbin@sandia.gov](mailto:jrobbin@sandia.gov)

**Pavel M. Chaplya**

Applied Mechanics Development  
Sandia National Laboratories  
Albuquerque, New Mexico, 87123

**ABSTRACT**

*Ferroelectric ceramics can be tailored at the microscale to have an ordered arrangement of crystal axes. Such grain-oriented ceramics can exhibit material properties far superior to conventional ceramics with random microstructure. A microstructurally based numerical model has been developed that describes the 3D non-linear behavior of ferroelectric ceramics. The model resolves the polycrystalline structure directly in the topology of the problem domain. The developed model is used to predict the effect of microstructural modifications on material behavior. In particular, we examine the internal residual stress after poling for idealized configurations of random and grain-oriented microstructures. The results indicate that a grain-ordered microstructure produces a significant increase in remanent polarization without detriment to internal residual stress.*

**INTRODUCTION**

Microstructurally engineered ferroelectric ceramics are tailored at the microscale to have an ordered arrangement of crystal axes. Such grain-oriented ceramics can exhibit material properties far superior to conventional ceramics with random microstructure. For example, lead-free ferroelectrics have been considered nonviable because of inferior single crystal properties. Carefully selected lead-free compositions can be processed with textured microstructure to compete directly with their lead-based counterparts [1, 2]. In addition to creating new ferroelectrics, and optimizing existing ferroelectrics, the ability to manipulate material microstructure enables the creation

of ceramic components specifically tailored for an application or device. However, when developing new ferroelectric materials (e.g., lead-free), or for optimization of existing materials, the need arises to evaluate the effect of microstructural modifications on bulk material response.

The present paper examines via numerical modeling the effect of microstructural tailoring on the internal stress that remains after poling. In what follows, the numerical model is described in brief, and the results of simulations on representative configurations are presented.

**NUMERICAL MODEL**

A microstructurally based numerical model has been developed that describes the 3D non-linear behavior of ferroelectric ceramics [3]. The model resolves the polycrystalline structure directly in the topology of the problem domain and uses the extended finite element method (X-FEM) to solve the governing equations of electromechanics. Each grain in the polycrystal is modeled as a single crystal with its own unique and randomly determined material basis. The material response is computed from anisotropic single crystal constants and the volume fractions of the polarization variants. Evolution of the variant volume fractions is governed by the minimization of internally stored energy and accounts for ferroelectric and ferroelastic domain switching in response to the applied loads.

## The Extended Finite Element Method for Electromechanics

The extended finite element method (X-FEM) is an extension of the classical FEM to treat functions with arbitrary discontinuities and discontinuous derivatives [4]. Interfaces are captured through a nodal enrichment function that, in this work, is based on a signed distance function.

In classical finite elements, geometric features are resolved in a conformal discretization so that the mesh must conform to external surfaces and internal interfaces. In many cases, such as with composite structures and multiple phase materials, it is a formidable task to create a conformal discretization. The X-FEM greatly simplifies the treatment of complex geometries by accommodating interfaces directly in the FEM interpolation thereby eliminating the need for conformal meshing.

The weak form of the governing equations of electromechanics, i.e., the conditions of mechanical and electrical equilibrium, is reduced to a discrete system of equations by the approximations

$$\mathbf{u}(\mathbf{x}) = \sum_I \mathbf{u}_I N_I(\mathbf{x}) + \sum_J \mathbf{a}_J N_J(\mathbf{x}) \eta(\mathbf{x}) \quad (1)$$

$$\phi(\mathbf{x}) = \sum_I \phi_I N_I(\mathbf{x}) + \sum_J \rho_J N_J(\mathbf{x}) \eta(\mathbf{x}) \quad (2)$$

where  $N_I(\mathbf{x})$  are the finite element shape functions, and  $\mathbf{u}_I$  and  $\phi_I$  are the nodal displacements and potential [4]. The first terms on the right hand side of equations 1 and 2 are the familiar finite element interpolation used in many conventional finite element codes. The second terms are due to the extended finite element method and accounts for the  $C^0$  continuity of an element that is bisected by an interface. In this term,  $\mathbf{a}_J$  and  $\rho_J$  are the *enrichment* degrees of freedom and exist only at those nodes whose support is intersected by an interface. The scalar valued function,  $\eta(\mathbf{x})$ , is referred to as the *enrichment function*. The enrichment function selected for this work was proposed by Moes [5] and is defined to be

$$\eta(\mathbf{x}) = \sum_I |\psi_I| N_I(\mathbf{x}) - \left| \sum_I \psi_I N_I(\mathbf{x}) \right| \quad (3)$$

where  $\psi_I$  are the nodal values of the level set representation of the boundary. The key feature of this function is that the first derivative is discontinuous. It is this attribute that makes the enriched interpolation of equations 1 and 2 well suited for elements with discontinuous derivatives.

In the present work, when voids are present in the problem domain, the X-FEM is used to capture the discontinuity of the free surface. Grain boundaries, however, are captured approximately by the classic finite element polynomial basis. Treating

the arbitrarily intersecting grain boundaries using the X-FEM is an ongoing effort.

## Constitutive Model

For the constitutive response, a micro-electromechanical material model is used that is similar to the one proposed by Huber [6] and used by Kamlah [7]. A more extensive description of the model used for this work can be found in [3].

A ferroelectric ceramic subjected to sufficiently large loads exhibits a nonlinear response due to the reorientation of electric dipoles and/or phase transitions. The nonlinearity of the material response is accommodated by decomposing the strain and electric displacement into their elastic (linear) and inelastic (nonlinear) parts;

$$\begin{aligned} \sigma_i &= c_{ij}^D \varepsilon_j^L - h_{ij} D_j^L \\ E_i &= -h_{ij} \varepsilon_j^L + \beta_{ij}^E D_j^L \end{aligned} \quad (4)$$

where

$$\begin{aligned} \varepsilon_i^L &= \varepsilon_i - \varepsilon_i^R \\ D_i^L &= D_i - D_i^R, \end{aligned} \quad (5)$$

and the inelastic quantities,  $\varepsilon_i^R$  and  $D_i^R$ , are a function of the load history. If there are  $n$  possible crystal variants, each variant can transition to every other variant, giving a possible  $n^2$  transition systems. Using the approach of Huber [6], the rate of change in volume fractions,  $\dot{c}^I$ , is related to the transition rate,  $\dot{\eta}$ , of active systems by a connectivity matrix,

$$\dot{c}^I = A^{I\alpha} \dot{\eta}^\alpha \quad (6)$$

where the summation on  $\alpha$  is implied and ranges from 1 to the number of transition systems,  $n^2$ . The numbering of the transition systems proceeds sequentially through the possible transitions from variant N to variant M for  $M = 1 \dots n, N = 1 \dots n$ . The connectivity matrix,  $A$ , is  $n \times n^2$ , wherein  $A^{I\alpha} = 1$  if activation of system  $\alpha$  increases  $c^I$ ,  $A^{I\alpha} = -1$  if activation of system  $\alpha$  decreases  $c^I$ , and  $A^{I\alpha} = 0$  if activation of system  $\alpha$  has no effect on  $c^I$ . The change in inelastic strain and electric displacement is computed according to  $\dot{\varepsilon}_{ij}^R = \varepsilon_{ij}^{R\alpha} \dot{\eta}^\alpha$  and  $\dot{D}_i^R = D_i^{R\alpha} \dot{\eta}^\alpha$  where  $\varepsilon_{ij}^{R\alpha}$  and  $D_i^{R\alpha}$  are the change in inelastic strain and electric displacement associated with transition system  $\alpha$ .

The increment of  $\eta^\alpha$  in a given load step is computed by

$$\Delta \eta^\alpha = -\tau(\mathbf{G}^\alpha - \mathbf{G}_c^\alpha). \quad (7)$$

The scaling parameter is given as  $\tau = (\sum_n \mathbf{H}^{nn})^{-1}$ , where  $n$  includes only active systems and

$$\mathbf{G} = \frac{1}{2} \mathbf{u} \mathcal{K}' \mathbf{u}^T + \mathbf{u}' \mathcal{K} \mathbf{u}^T \quad (8)$$

$$\mathbf{H} = \mathbf{u}' \mathcal{K} \mathbf{u}^T + 2 \mathbf{u}' \mathcal{K}' \mathbf{u}^T \quad (9)$$

where

$$\mathbf{u} = [\mathbf{\epsilon}_ij^L \mathbf{D}_i^L] \quad (10)$$

$$\mathbf{u}' = [-\mathbf{\epsilon}_ij^{R\alpha} - \mathbf{D}_i^{R\alpha}] \quad (11)$$

$$\mathcal{K} = \begin{bmatrix} C_{ijkl} & -h_{ijk} \\ -h_{ijk} & \beta_{ij} \end{bmatrix} \quad (12)$$

$$\mathcal{K}' = \begin{bmatrix} C_{ijkl}^I A^{I\alpha} & -h_{ijk}^I A^{I\alpha} \\ -h_{ikl}^I A^{I\alpha} & \beta_{ik}^I A^{I\alpha} \end{bmatrix}. \quad (13)$$

The critical energy level required for activation of each transition system is given by

$$\mathbf{G}_c^\alpha = -\sigma_{ij}^c \mathbf{\epsilon}_{ij}^{R\alpha} - E_i^c \mathbf{D}_i^{R\alpha}. \quad (14)$$

where  $\sigma_{ij}^c$  and  $E_i^c$  are the coercive stress and coercive fields, respectively. Once  $\eta^\alpha$  are computed, the updated values of the bin fractions,  $c^I$ , inelastic strain,  $\mathbf{\epsilon}_{ij}^R$ , and inelastic polarization,  $\mathbf{D}_i^R$ , are computed.

## RESULTS

The above model is applied to a hypothetical rhombohedral ferroelectric polycrystal (see table 1). The polycrystalline structure is idealized using a Voronoi decomposition of the problem domain into 16 grains. Samples are either fully dense or porous, and have aligned or random material bases, resulting in four configurations. The porous sample has a single pore at the origin resulting in a porosity of approximately two percent. Samples with aligned material bases have the [111] direction of each grain aligned with the global z axis, but rotation about this axis is randomly selected.

Table 1. RHOMBOHEDRAL MATERIAL CONSTANTS.

Elastic stiffness, $c_{11}$	$1.491 \times 10^{11} \text{ Pa}$
$c_{12}$	$7.109 \times 10^{10} \text{ Pa}$
$c_{13}$	$5.347 \times 10^{10} \text{ Pa}$
$c_{33}$	$1.107 \times 10^{11} \text{ Pa}$
$c_{44}$	$2.642 \times 10^{10} \text{ Pa}$
Relative permittivity, $\epsilon_{11}$	145.0
$\epsilon_{33}$	335.0
Piezoelectric constant, $h_{33}$	$3.91 \times 10^8 \text{ N/C}$
$h_{31}$	$1.32 \times 10^8 \text{ N/C}$
$h_{24}$	$1.41 \times 10^8 \text{ N/C}$
Lattice parameter, $a$	4.148 Å
Lattice parameter, $\alpha$	1.566
Spontaneous polarization	$0.37 \text{ C/m}^2$

There are eight crystal variants in a rhombohedral ferroelectric, one for each body diagonal of the unit cell, resulting in 64 possible transition systems. The transition strains and transition polarizations are computed as the respective differences in spontaneous strain and spontaneous polarization between variants.

Each configuration is subjected to a polarizing electric field of  $3.0 \text{ MV/m}$  along the x axis, perpendicular to the alignment axis. To accommodate domain switching events without limiting the load step throughout the calculation, zeroth order parameter continuation is used so that the maximum change in electric displacement magnitude remains within specified limits.

The electrical response of the aligned and random configurations is shown in figures 1 and 2. As could be expected, in both the porous and solid configurations the aligned samples achieve a significantly higher remanent polarization (11 percent and 15 percent, respectively) due to the alignment of the [111] material axis.

The electrical response in figures 1 and 2 is a measure of bulk material response. Perhaps the most useful aspect of spatially and temporally resolved numerical modeling is the ability to examine local fields. In an effort to quantify the local internal residual stresses, figures 3 and 4 show plots of the volume fraction of material at a given von Mises stress after the polarizing field has been removed. In the figure, the points are the actual numerical value and the solid lines are a gaussian fit to assist the eye. The peak residual stresses in the samples do not appear to be greatly affected by the microstructural modification, however, the median von Mises stress decreases appreciably in the aligned samples.

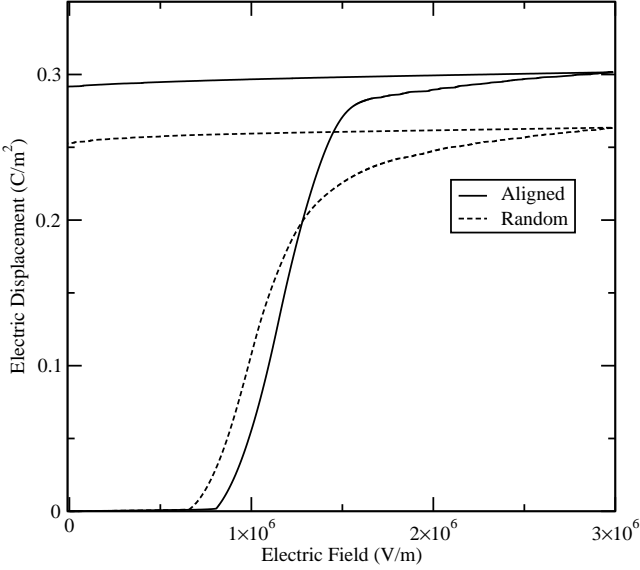


Figure 1. CALCULATED ELECTRICAL RESPONSE OF ALIGNED AND RANDOM SOLID MICROSTRUCTURES TO POLARIZING FIELD.

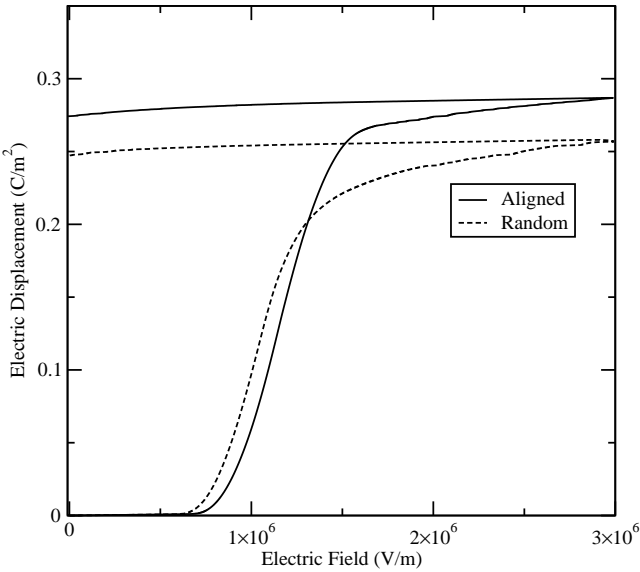


Figure 2. CALCULATED ELECTRICAL RESPONSE OF ALIGNED AND RANDOM POROUS MICROSTRUCTURES TO POLARIZING FIELD.

Figures 5 and 6 represent the domain configuration for both the aligned and random configurations after poling. The poling direction is at  $\theta = 0$ , i.e., the positive x axis in the figure. The polar coordinate is the angle from the poling direction, and the radial coordinate indicates the *domain fraction*, the ratio of current to initial (unpoled) values of the material volume whose

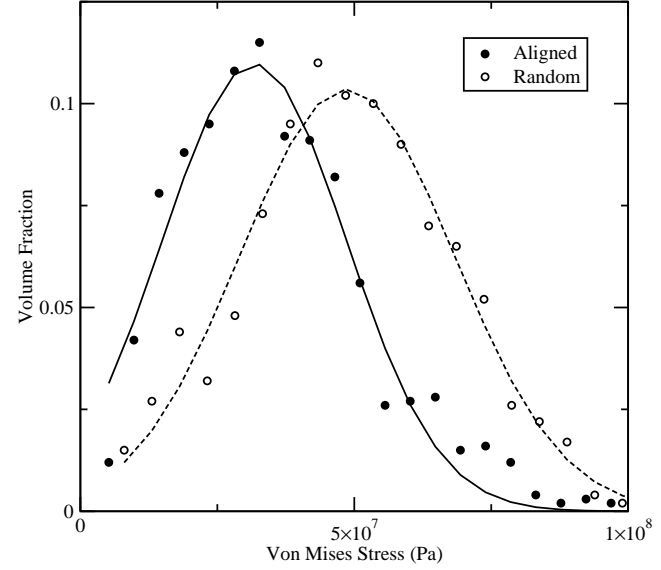


Figure 3. CALCULATED RESIDUAL STRESS DISTRIBUTION IN ALIGNED AND RANDOM SOLID MICROSTRUCTURES AFTER BEING SUBJECTED TO POLARIZING FIELD.

spontaneous polarization lies within the given range of angles. For an unpoled sample, the polar plot has a value of one at all angles. For a typical poled sample, the polarization dipoles will be distributed about the poling direction with the majority falling within  $45^\circ$ . In the random configurations a significant amount of material remains laterally oriented to the poling direction. However, the aligned samples achieves a superior alignment with the poling axis and yields a significantly higher remanent polarization.

## CONCLUSIONS

A spatially resolved numerical model is used to examine the effect of a tailored microstructure on remanent polarization and internal residual stress after poling of a hypothetical rhombohedral ferroelectric polycrystal. By aligning the [111] material direction with the global z axis the remanent polarization that can be achieved on an axis perpendicular to the alignment axis increases significantly. The numerical results indicate that this improvement in remanent polarization is without penalty in terms of the internal residual stresses introduced during poling.

## ACKNOWLEDGMENT

Sandia is a multiprogram laboratory operated by Sandia Corporation, a Lockheed Martin Company, for the United States Department of Energy's National Nuclear Security Administration under contract DE-AC04-94AL85000.

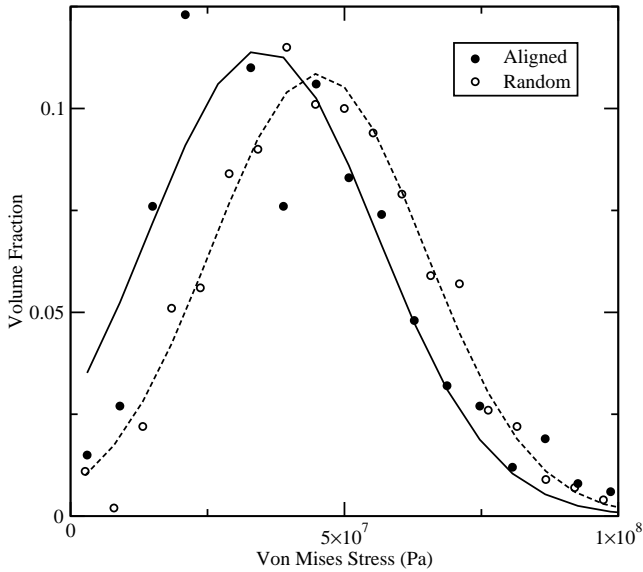


Figure 4. CALCULATED RESIDUAL STRESS DISTRIBUTION IN ALIGNED AND RANDOM POROUS MICROSTRUCTURES AFTER BEING SUBJECTED TO POLARIZING FIELD.

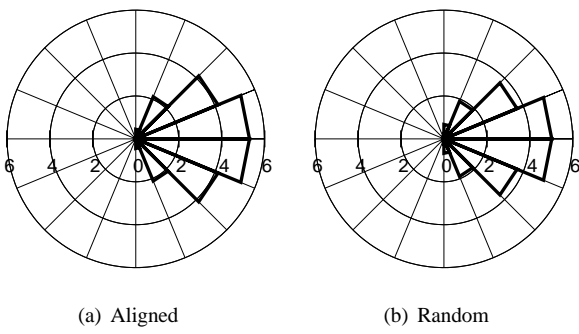


Figure 5. POLAR PLOTS OF THE RELATIVE DOMAIN FRACTIONS AFTER POLING THE SOLID CONFIGURATIONS.

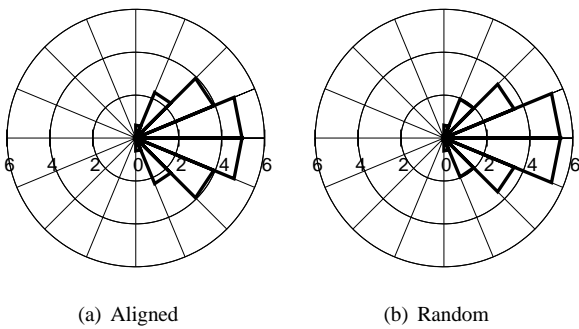


Figure 6. POLAR PLOTS OF THE RELATIVE DOMAIN FRACTIONS AFTER POLING THE POROUS CONFIGURATIONS.

## REFERENCES

- [1] Tani, T., and Kimura, T., 2006. "Reactive-templated grain growth processing for lead free piezoelectric ceramics". *Advances in Applied Ceramics*, **105**(1), February, pp. 55 – 63.
- [2] Saito, Y., Takao, H., Tani, T., Nonoyama, T., Takatori, K., Homma, T., Nagaya, T., and Nakamura, M., 2004. "Lead-free piezoceramics". *Nature*, **432**(7013), Nov, pp. 84 – 87.
- [3] Robbins, J., Khraishi, T. A., and Chaplya, P. M., 2007. "Microstructural modeling of ferroic switching and phase transitions in pzt". *Proceedings of SPIE - The International Society for Optical Engineering*, **6526**, Apr.
- [4] Belytschko, T., Parimi, C., Moes, N., Sukumar, N., and Usui, S., 2003. "Structured extended finite element methods for solids defined by implicit surfaces.". *International Journal for Numerical Methods in Engineering*, **56**(4), Jan, pp. 609 – 35.
- [5] Moes, N., Cloirec, M., Cartraud, P., and Remacle, J. F., 2003. "A computational approach to handle complex microstructure geometries.". *Computer Methods in Applied Mechanics and Engineering*, **192**(28/30), Jul, pp. 3163 – 77.
- [6] Huber, J. E., Fleck, N. A., Landis, C. M., and McMeeking, R. M., 1999. "A constitutive model for ferroelectric polycrystals.". *Journal of the Mechanics and Physics of Solids*, **47**(8), pp. 1663 – 97.
- [7] Kamlah, M., Liskowsky, A. C., McMeeking, R. M., and Balke, H., 2005. "Finite element simulation of a polycrystalline ferroelectric based on a multidomain single crystal switching model.". *International Journal of Solids and Structures*, **42**(9/10), May, pp. 2949 – 64.